Available online at www.sciencedirect.com

ScienceDirect

Procedia Structural Integrity 2 (2016) 409–416

Structural Integrity Procedia

www.elsevier.com/locate/procedia

21st European Conference on Fracture, ECF21, 20-24 June 2016, Catania, Italy

Numerical analysis of the geometrical and material criteria of acceleration of shear crack to supershear velocity in brittle nanoporous solids

Evgeny V. Shilko[a]*, Sergey G. Psakhie[a], Valentin L. Popov[b]

[a]*Institute of Strength Physics and Materials Science SB RAS (ISPMS SB RAS), 2/4, pr. Akademicheskii, 634055 Tomsk, Russia*
[b]*Berlin University of Technology (TU Berlin), Sekr. C 8-4, Str. Des 17. Juni 135, D-10623 Berlin, Germany*

Abstract

The paper is devoted to the study of dynamic propagation of mode II cracks in porous brittle materials with nanoscale pore size. We compared static (shear strength) and dynamic parameters of crack growth in dry and fluid saturated nanoporous brittle materials at different degrees of confinement. We have shown that pore fluid in nanoporous brittle materials influences mainly the dynamics of crack propagation. This leads in particular to pronounced peculiarities of the dependence of the critical value of dimensionless geometrical parameter of the initial crack (it majorizes the interval of the ratios of length to thickness for the cracks that are capable to accelerate to intersonic velocity) on applied crack normal stress. The results of the study are relevant for understanding the conditions of supershear regime of propagation of mode II cracks as well as for assessment of the ability of mode II cracks in brittle materials (including nanoporous fluid-saturated solids) to develop in supershear regime.

Keywords: brittle solid; mode II crack; sub-Rayleigh-to-supershear transition; fluid; pore pressure; modeling; hybrid cellular automata method

1. Introduction

The conditions defining the regime and, in particular, the velocity of dynamic propagation of longitudinal shear (mode II) cracks in brittle materials are widely studied and analyzed over the past few decades. Considerable interest in this subject is concerned with its close connection with the problems of fracture of multiphase materials, the

* Corresponding author. Tel.: +7-382-228-6971; fax: +7382-249-2576.
E-mail address: shilko@ispms.tsc.ru

10.1016/j.prostr.2016.06.053

dynamics of earthquakes and seismic radiation, as well as a common problem of initiation and possible regimes of dynamic slip of contact surfaces (Barras et al. (2014), Svetlizky et al. (2016)). An important feature of dynamic propagation of mode II cracks is shear stress concentration in the vicinity of the crack tip (Broberg (2006)).

Beginning with the classical papers of works Burridge (1973) and Andrews (1976), we know that the initial stage of dynamic crack growth is accompanied by shear stress concentration in a compact area ahead of the crack tip (this is a so-called stress peak). In recent decades, the evolution of the stress peak became a subject of a number of studies, mainly due to the fact that it is supposed to be responsible for the formation of supershear (another name is intersonic) secondary cracks that are capable to propagate at velocities V above the shear elastic wave speed V_S and below the P-wave speed V_P. In particular, it has been shown in Shilko and Psakhie (2014) and Psakhie et al. (2015) that the physical mechanism for the formation of a compact area with high shear stresses ahead of the tip of dynamically growing mode II crack is the nucleation and development of the collective elastic vortex-like motion (hereinafter called the elastic vortex). These studies have shown that the elastic vortex is scale-invariant dynamic object, an important feature of which is the concentration of shear stress. The maximum attainable magnitude of the shear stress in the elastic vortex is the unequivocal function of the dimensionless geometrical parameter P of the initial crack. There is a critical value (P_{crit}) of this parameter, such that if $P<P_{crit}$, the initial interface crack is able to propagate at supershear velocity ($V>V_S$). Otherwise, it is able to distribute only in conventional sub-Rayleigh regime ($V<V_R$). Shilko et al. (2015) have shown that the specific value of P_{crit} is determined by the material parameters. Note that stress concentration in elastic vortices is able to promote not only crack acceleration but inelastic deformation including dynamic migration of grain boundaries (Psakh'e and Zol'nikov (1997)).

The results obtained in Shilko and Psakhie (2014), Psakhie et al. (2015) and Shilko et al. (2015) refer to the conditions of simple shearing of brittle materials including porous and fissured brittle materials of natural and artificial origins (ceramics, rocks). Pronounced features of the mechanical response of such materials are a significant influence of the value of normal load on shear strength (this feature is inherent to all brittle solids) as well as an important role of fluid pressure and redistribution in the pore space. Among porous materials a subclass of materials with nanoscale pore structure can be distinguished. An important feature of the nanoporous permeable materials is a determining role of adsorption effects, manifested, in particular, in the existence of a threshold (minimum) value of the pore pressure at which the liquid can filtrate in the pore space of the material. The estimates with use of the typical values of parameters for «sandstone-water» system with nanoscopic characteristic pore size in sandstone (<0.01 μm) show that threshold pore pressure of fluid may reach several tens of megapascals, that in many cases comparable to the strength of porous materials themselves. Therefore, at relatively low mean stresses mechanical deformation of fluid saturated nanoporous materials is not accompanied by fluid redistribution in the pore space (or filtration power is negligibly slow). In this case the material with interconnected nanoscopic pores and channels behaves in much the same way as materials with isolated pores.

Influence of pore fluid pressure on the mechanical properties and fracture of brittle porous materials is the subject of extensive theoretical and experimental studies carried out by various authors (Bidgoli and Jing (2014), Ougier-Simonin and Zhu (2015)). Due to relatively low values of cohesion in brittle materials the special emphasize is laid on the study of the shear strength and dynamics of growth of longitudinal shear cracks as well as their relationship with the magnitude of the applied crack normal load and pore pressure (Radi and Loret (2007), Brantut and James (2011)). This problem was the subject of the present research as it applied to nanoporous materials.

2. Problem statement

The study was carried out on the basis of numerical modeling using hybrid cellular automata method. The formalism is this method couples mathematical formalisms of movable cellular automata method, which belongs to a group of discrete element methods, and finite difference method (Psakhie et al. (2016)). The study of the dynamic growth of mode II cracks was carried out in the framework of the macroscopic consideration of the material. The pore structure of materials and interstitial fluid (liquid) were implicitly taken into account through the parameters of the models of mechanical response of fluid saturated porous solid and interstitial fluid. The influence of pore fluid pressure on the stress state of the solid skeleton was described using Biot's model of poroelasticity. We considered a model nanoporous macroscopically isotropic linear-elastic (brittle) material with porosity 10% and characteristic pore size d_{ch} < 0.01 μm. Two-parametric criterion of Drucker and Prager was used as a fracture criterion.

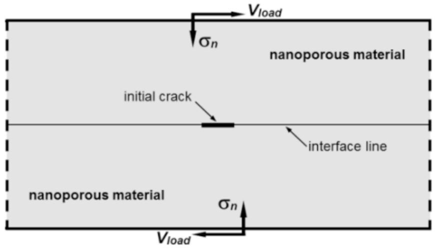

Fig. 1. Schematic and the loading scheme of two-dimensional model slab made from nanoporous brittle material. The slab consists of two parts bonded by low-strength interface. Vertical dashed bold lines delineate the vertical faces to which periodic boundary conditions in the horizontal direction are applied. Preliminary stress state is defined by applying vertical (normal to the interface line) compressive stress σ_n to the upper and lower boundaries of the slab and subsequent (after the establishment of stationary stress state) fixing their vertical positions. Longitudinal shear loading is modeled by horizontal displacement of the upper and lower external boundaries in opposite directions at small constant velocity V_{load}.

Typical elastic and strength parameter of porous (~10%) sandstones were used as parameters of model material (note that material parameters of some porous ceramic materials are close to typical parameters of sandstones).

We modelled two-dimensional model rectangular samples (long slabs), which consist of two bonded parts, in the plane-strain-state approximation (Fig. 1). Parts have the same properties and are isotropic, poroelastic and high-strength. Ideal bonding between the parts was assumed (applied model is analogous to the model of infinitely thin cohesive zone). Interface strength was taken to be much smaller than the strength of material of the plates. An initial crack is introduced at the interface. Preliminary stress state of the samples was set by applying vertical compressive load to the upper and lower surfaces. Longitudinal shear was realized by displacing the upper and lower surfaces of the pre-stressed sample in the horizontal direction at low velocity (Fig. 1). Such loading conditions correspond to confined longitudinal shear. One of the main characteristics of confined shear is the value of pressure on the upper and lower surfaces of the sample, namely the crack (and interface) normal stress σ_n.

Under described loading conditions the initial interface crack begins to dynamically propagate along the interface line (straight line) when the applied shear stress reaches a threshold (a shear strength τ_0 of the system with the initial crack; τ_0 amounts some fraction of shear strength of intact interface at assigned value of normal load σ_n).

Hydrostatic compression of fluid saturated (in this study, water-saturated) material is accompanied by growth of pore pressure p_{pore}, which has a significant impact on the stress state and strength of solid skeleton. In classical models of fluid-saturated porous materials this effect is taken into account through the formulation of Hooke's law and fracture criterion in terms of so-called effective stresses instead of "mechanical" stresses induced by applied load. In the framework of this approximation the presence of fluid in the pore space changes volumetric stresses in the skeleton. It is known that the stress state of the material in the vicinity of initial crack as well as ahead of the crack dynamically growing in sub-Rayleigh regime is complex and includes significant volumetric component even under the condition of applied simple shear deformation. Hence stress and strain distribution ahead of the mode II crack will be largely determined by pore pressure, which, in turn, is determined by the applied crack normal stress σ_n. Therefore, in the present study we have done a comparative analysis of the characteristics of dynamic crack propagation in dry and fluid saturated nanoporous materials under at different values of applied crack normal stress.

3. Simulation results and discussion

3.1. "Dry" brittle porous material

The results of the simulation showed common dynamics of unstable crack growth for different degrees of material confinement characterized by the magnitude of σ_n. In the initial stage of crack growth a collective elastic vortex-like motion of material points in the region ahead of the crack tip (elastic vortex, Fig. 2,a-c) is nucleated and developed. A characteristic feature of the elastic vortex is concentration of shear stress (in other words, concentration of elastic shear strain energy density) in its frontal part. The source of the elastic strain energy in the elastic vortex is its inflow from the unloaded parts of the slab behind the crack tip. During the course of dynamic propagation of a crack the elastic vortex increases in size, and the concentration of shear stresses in its frontal part gradually increases (Fig. 2,d-f). The velocity of steady motion of the elastic vortex is equal to shear wave speed in the material, while the crack develops at a velocity lower than Rayleigh wave speed and hence less than velocity of the vortex. Therefore during the course of propagation the elastic vortex gradually moves away from the tip and finally detaches from it. After detachment the elastic vortex becomes a self-dependent dynamically propagating object (Psakhie et al. (2015)). The widely studied phenomenon of acceleration of dynamically propagating crack towards the velocities comparable to the longitudinal wave speed V_P in the material takes place, if magnitude of shear stresses in the vortex reaches the value of the shear strength of intact interface prior to detachment of the vortex from the crack tip. In this case the secondary rupture nucleates at the interface ahead of the crack tip (in the frontal part of the vortex). This secondary rupture propagates at a velocity higher than the shear wave speed (Fig. 3).

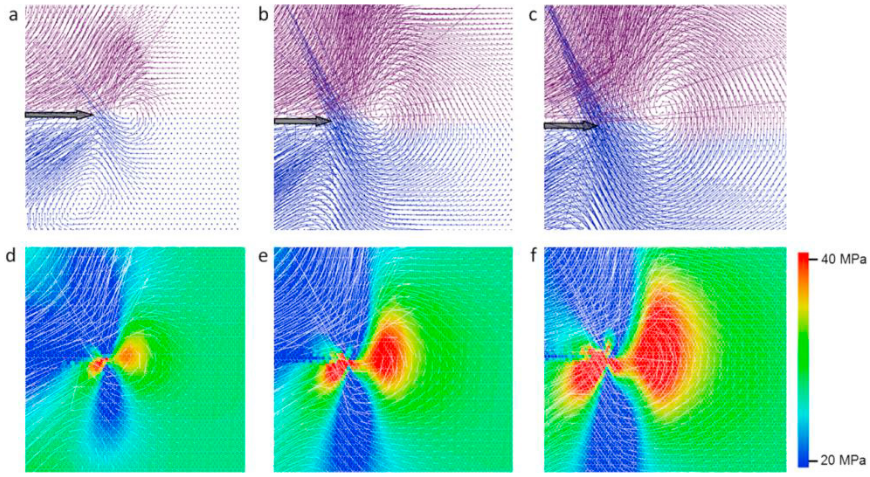

Fig. 2. Snapshots of the velocity field (a-c) and the distribution of equivalent stress (d-f) near the tip of a growing longitudinal shear crack 1.5 μs (a,d), 4.5 μs (b,e) and 7.5 μs (c,f) after the beginning of propagation. The horizontal arrows mark the position of the plane of the crack and of its right tip. The white lines in (d-f) depict particle velocities.

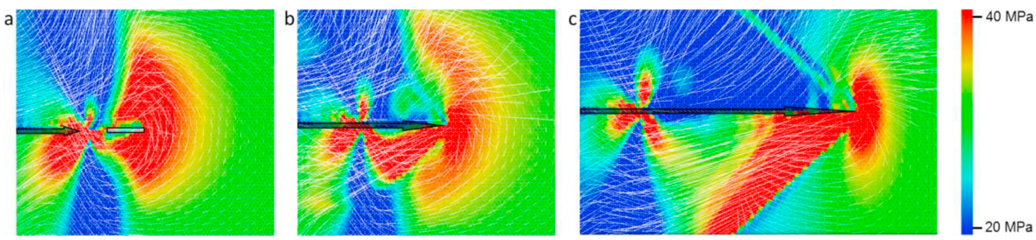

Fig. 3. Snapshots of the distribution of equivalent stress near the tip of a propagating crack 0.2 μs (a), 1.0 μs (b) and 3.6 μs (c) after the moment of nucleation of the secondary crack at a small distance ahead of the main crack.

The results of theoretical and experimental researches carried out by various authors show that dynamic crack propagation in a steady state regime can be considered as a scale invariant process. Therefore, the conditions of the beginning of dynamic crack growth and crack propagation dynamics (including sub-Rayleigh-to-supershear transition) are determined by the intensive (specific) characteristics of the system. Results of previous study by the authors of this paper have shown that initial crack is potentially able to propagate in supershear regime under longitudinal shear loading if the shear strength τ_0 of the system with a crack exceeds certain critical value. Shear strength τ_0 of the slab with initial interface crack is determined, apart from material parameters, by geometrical characteristic of a crack. In view of the scale invariance of the crack propagation dynamics, this characteristic should be dimensionless combinations of dimensional characteristics of a crack. Psakhie et al. (2015) proposed such a parameter for straight cracks. It is a ratio of initial crack length L to crack effective thickness D: $P=L/D$. Under the condition of simple shear loading the value of τ_0 is an unequivocal function of dimensionless parameter P.

The results of the present study have shown that under the condition of confined shearing the value of shear strength τ_0 is an increasing function of crack normal stress σ_n. On the basis of these results we have built a general functional form of the dependence of the shear strength τ_0 of brittle material with an initial crack on the dimensionless geometrical characteristics P of the crack for different values of crack normal stress σ_n (Fig. 4,a):

$$\tau_0 = \tau_{is}(\sigma_n)\sqrt{\frac{1}{1+\alpha(\sigma_n)P}\left(1-\left(\frac{\tau_\infty(\sigma_n)}{\tau_{is}(\sigma_n)}\right)^2\right)+\left(\frac{\tau_\infty(\sigma_n)}{\tau_{is}(\sigma_n)}\right)^2}\,, \tag{1}$$

where τ_{is} is the shear strength of intact interface at the assigned value of σ_n, τ_∞ is the shear strength of the interface with semi-infinite crack, α is a dimensionless parameter, which depends on material properties as well as on the normal stress σ_n. Special study have shown that τ_∞ is an increasing function of σ_n, while α decreases with σ_n increase. The function $\tau_{is}(\sigma_n)$ for plain strain state is derived analytically on the basis of Hooke's law:

$$\tau_{is}(\sigma_n)=\sqrt{\frac{1}{3}\left[\frac{[\sigma_c + a\sigma_n(1+\nu)/(3(1-\nu))]^2}{b^2}-\sigma_n^2\left(\frac{1-2\nu}{1+\nu}\right)^2\right]}\,. \tag{2}$$

Here $a=1.5(\sigma_c/\sigma_t-1)$ and $b=0.5(\sigma_c/\sigma_t+1)$ are parameters of applied fracture criterion of Drucker and Prager (σ_c and σ_t are uniaxial compression strength and tensile strength of dry material), ν is a Poisson's ratio. Under the condition of simple shear (σ_n=0): $\tau_\infty \approx 0.1\tau_{is}$, $\alpha=\alpha_0(1-\nu)\sqrt{1+\nu}$, $\alpha_0 \approx 0.55$ (Psakhie et al. (2015)).

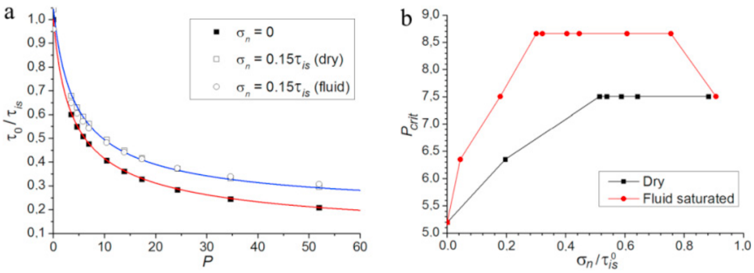

Fig. 4. (a) examples of the dependences of the shear strength τ_0 of dry and fluid saturated nanoporous samples with initial interface crack on the value of dimensionless geometrical crack parameter P at different values of applied crack normal stress σ_n (each series of points at certain value of σ_n is normalized to the value of shear strength of the intact interface τ_{is} at σ_n); (b) dependences of P_{crit} on applied crack normal stress σ_n (which is normalized to the value of shear strength of intact interface under the condition of simple shear) for dry and fluid saturated samples.

Main differences between curves $\tau_0(P)$ at different values of σ_n are connected with increasing the shear strength of the interface with semi-infinite crack as σ_n increases. This can be explained by complex stress state of tip of the initial crack under the condition of longitudinal shear. This stress state includes crack normal tensile stress. Therefore shear deformation is accompanied by crack opening. Maximum crack opening displacement is in its central part. Contribution of tensile stresses (and hence the crack opening displacement) increases with increase in the value of dimensionless geometrical crack parameter P. This determines nonlinear decrease in shear strength (Fig. 4,a). Contribution of tensile stress to stress state in the vicinity of the crack tip decreases with increase in the normal stress σ_n. Accordingly, crack opening displacement is reduced down to zero. At large values of σ_n crack surfaces remain in a compressed state until the beginning of dynamic crack growth. The above explains increase in shear strength τ_0 with σ_n at the same value of P. Therefore increase in σ_n leads to gradual and nonlinear "flattening" of the dependence $\tau_0(P)$. Note that empirically derived expression (1) is a generalization of the conventional Griffith expression as it is valid for different scale cracks being under the condition of confined longitudinal shear loading.

Simulation results showed that the maximum shear stress in the elastic vortex (at the moment of vortex separation from dynamically growing crack) is a linear function of the shear strength of the system with the initial crack τ_0. In view of (1) such a relationship suggests the existence of a critical value of the parameter P=P_{crit}. If the initial crack is characterized by the magnitude of the dimensionless parameter P<P_{crit}, during the course of dynamic crack propagation the magnitude of shear stress in the elastic vortex reaches the shear strength of the interface before the moment of detachment. Such initial cracks can, in principle, overcome the Rayleigh wave velocity barrier. At the same time initial cracks characterized by parameters P>P_{crit}, can only propagate at velocities below the Rayleigh wave speed. Since shear strength of brittle materials depend on mean stress, the value of P_{crit} is a function not only of the material parameters (Shilko et al. (2015)), but also the value of σ_n. Results of the study have shown that the dependence $P_{crit}(\sigma_n)$ is a non-linear increasing function (Fig. 4,b), which tends to saturation (P_{crit}^{limit}) at the values of σ_n close to the half the value of interface shear strength τ_{is}^{0} under the condition of simple shear (σ_n=0).

3.2. Fluid saturated brittle porous material

Within the framework of the approximations of neglecting filtration processes in fluid-saturated nanoporous brittle materials a key determinant of mechanical properties of nanoporous materials and features of dynamic processes in them is the pore fluid pressure p_{pore}. Results of the study have shown that under the condition of confined longitudinal shear the stress state of fluid saturated nanoporous material significantly differs from stress state of dry material. As an example, Fig. 5 shows mean stress distribution in dry and fluid saturated slabs near the right tip of the initial crack in the limiting state (to the moment of the beginning of dynamic crack growth). One can see that the presence of the fluid leads to a "long-range" compressive stress fields near the crack tip (the length of the blue area in Fig. 5,b is several times greater than the length of a similar area in Fig. 5,a). The dimensions of the "unloading" region near the crack tip, where mean stress values are small and may even be positive, are reduced as well. At the same time differences in the distribution of equivalent stress near the crack tip in the limiting state in dry and fluid saturated samples (at the same value of σ_n) are insignificant. Thus, we can state that elastic strain energy density ahead of the crack tip in fluid saturated nanoporous solid is significantly higher, mainly due to increase in the contribution volume strain energy. Nevertheless, differences in stress states of the dry and fluid saturated nanoporous materials in the tip of the initial crack are much less significant. The consequence of this is that the main distinctions of fluid saturated nanoporous material with crack relate to the dynamics of crack growth, whereas the static properties (including shear strength) insignificantly differ from dry material.

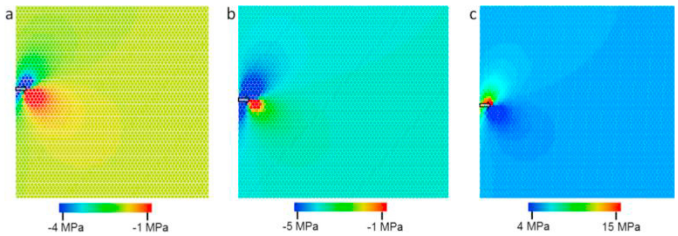

Fig. 5. Examples of means stress (a,b) and pore pressure (c) distribution in dry (a) and fluid saturated (b,c) samples of nanoporous material in the limiting state (at the moment of the beginning of propagation of the initial crack). In both examples σ_n=0.15 τ_{is}^{0} .

The simulation results showed indeed that dependences of shear strength τ_0 of fluid saturated samples with interface cracks on the dimensionless geometrical crack parameter P at various values of applied normal stress σ_n are close to corresponding curves $\tau_0(P)$ for dry samples (Fig. 4,a). Similar to dry material, empirically determined dependences $\tau_0(P)$ for fluid saturated nanoporous material are approximated well by the empirical expression (1). At the same time, though dependences $\alpha(\sigma_n)$ and $\tau_\infty(\sigma_n)$ for dry and fluid saturated materials differ insignificantly (α decreases, while τ_∞ increases with σ_n), dependences $\tau_{is}(\sigma_n)$ have opposite trends. Shear strength of intact interface τ_{is} in dry slab gradually linear increases with σ_n, while gradually linear decreases in fluid saturated slab. The absolute values of slopes of these linear dependences are close to each other. Note that the absolute value of the slope of the dependence $\tau_{is}(\sigma_n)$ is insignificant. In the shown example increase in the value of σ_n from 0 up to τ_{is}^0 is accompanied by change in the magnitude of τ_{is} within 25%. Specific values of parameters of the dependences $\alpha(\sigma_n)$, $\tau_\infty(\sigma_n)$ and $\tau_{is}(\sigma_n)$ are determined by material porosity as well as by the ratio of fluid bulk modulus to the bulk modulus of the material constituting solid skeleton.

Described features of the stress state of fluid saturated porous materials (namely, the formation of an extensive area with high compressive stress) near the crack tip define peculiarities of dynamic crack growth under the conditions of confined longitudinal shear. Fig. 6 shows examples of the dynamics of mean stress evolution near the right tip of dynamically growing crack in dry and fluid saturated nanoporous material. One can see that the boundary of the area with high compressive stresses (blue area in Fig. 6,a,b) in dry slab is confined to the crack front and propagates at the same velocity as the crack tip. At the same time such boundary in fluid saturated material propagates at the longitudinal elastic wave speed, which is much faster than crack velocity (Fig. 6,c,d). Analysis of the simulation results shows that this is due to the dynamic changes in pore fluid pressure ahead of moving crack tip. Thus, the integral energy flux to the region ahead of the tip of dynamically growing crack in fluid saturated medium is larger due to larger contribution of volume strain energy flux. One consequence of this is slightly larger crack propagation velocity in sub-Rayleigh regime. Although this increase is small (a few percent), but it has a significant impact on the critical values of the energy and geometric parameters that determine the ability of a longitudinal shear crack to propagate in supershear regime. In particular, the critical density of elastic strain energy accumulated in the system to the moment of the beginning of the crack growth is reduced, and corresponding critical value of geometrical crack parameter P_{crit} increases as compared with confined dry material.

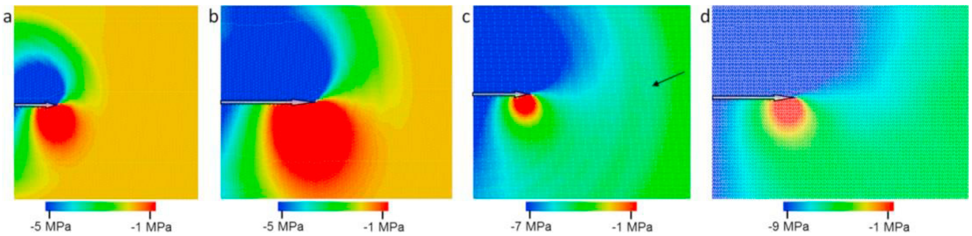

Fig. 6. Snapshots of the distribution of mean stress near the tip of a propagating sub-Rayleigh crack in dry (a,b) and fluid saturated (c,d) samples of nanoporous material (σ_n=0.15 τ_{is}^0 , P=5.8). Black inclined arrow in (c) shows the front of strong solitary P-wave (compression wave) initiated by pore pressure change ahead of the crack tip.

Dependence of P_{crit} on the magnitude of applied normal stress σ_n is a nonmonotonic function, which quickly reaches a maximum and then (at the values of σ_n approaching τ_{is}^0) decreases to a value P_{crit}^{limit} (Fig. 4b). Thus, at "high" degrees of confinement ($\sigma_n \to \tau_{is}^0$) the critical value of dimensionless geometrical parameter of the initial crack is the same for dry and fluid saturated brittle materials. This is due to the fact that at high crack normal compression stresses distortion of stress field near the crack tip diminishes. As we noted above, these distortions are significantly different in dry and fluid saturated materials. In the latter case there is an extensive area with high compressive mean stresses ahead of the crack. Higher elastic strain energy density in this area provides a greater intensity of energy flow from the crack to the elastic vortex at the initial stage of dynamic crack propagation and, consequently, faster growth of stresses in the elastic vortex. Therefore, rate of increase of P_{crit} at relatively low values of σ_n in fluid saturated material is more than two time higher than in dry material (larger P_{crit} means longer or thicker cracks, that are capable to propagate in supershear regime). Increase in the value of σ_n is accompanied by decrease in the dimensions of the area with high compressive mean stresses ahead of the tip of initial crack. This leads, at first, to the saturation of P_{crit}, and then to its small decrease to a value of P_{crit}^{limit} (at high σ_n stress states of dry and fluid saturated materials ahead of the initial crack are much closer to each other).

The most pronounced peculiarity the dynamics of longitudinal shear crack propagation in fluid saturated nanoporous material is the value of crack propagation velocity in supershear regime. For the considered model saturated fluid material it is more than 30% higher than in dry material (although the differences between the values of crack propagation velocity in the sub-Rayleigh regime do not exceed a few percent). The absolute value of the difference between supershear crack propagation velocities in dry and fluid saturated brittle materials is determined by the porosity and the ratio of fluid bulk modulus to bulk modulus of the material of solid skeleton.

4. Conclusion

The study showed that the pore fluid in nanoporous brittle materials influences mainly the dynamic properties of longitudinal shear cracks, while static properties (including shear strength) of the material with initial crack are much sensitive to the presence of pore fluid. The main peculiarity of the dynamic properties of the cracks in preliminary stressed fluid saturated nanoporous material is nonmonotonic dependence of critical value of dimensionless geometrical crack parameter (it characterizes limiting values of length and thickness of the cracks, that are capable to accelerate to intersonic velocity) on applied crack normal stress. This dependence has a maximum at relatively low values of crack normal stress and then decreases to limiting value, which coincide with limiting value for dry material.

It should be noted that above described features are specific for nanoporous materials. Special study has shown that the revealed regularities of dynamic growth of shear cracks in the fluid saturated permeable materials with characteristic pore sizes amounting to a few tenths of a micrometer are close to the same for dry materials (excluding the velocity of supershear crack propagation). The results suggest a complex and non-linear influence of fluid phase, which cannot be imitated using external mechanical loading of dry brittle material.

It is known that the character of the mechanical response of brittle solids gradually change from brittle to ductile at sufficiently large values of compressive mean stress, which are close to and higher than the magnitude of the unconfined shear strength of the material (Wong and Baud (2012)). Therefore, the present consideration was limited by the range of relatively small mean stresses that are not enough for ductile fracture of brittle materials.

Acknowledgements

The authors thank the Russian Science Foundation (Project 14-19-00718) for financial support.

References

Andrews, D.J., 1976. Rupture Velocity for Plane Strain Shear Cracks. Journal of Geophysical Research 81, 5679–5687.

Barras, F., Kammer, D.S., Geubelle, P.H., Molinary, J.-F., 2014. A Study of Frictional Contact in Dynamic Fracture Along Bimaterial Interfaces. International Journal of Fracture 189, 149–162.

Bidgoli, M.N., Jing, L., 2014. Water Pressure Effects on Strength and Deformability of Fractured Rocks Under Low Confining Pressures. Rock Mechanics and Rock Engineering 48, 971–985.

Brantut, N., Rice, J.R., 2011. How pore fluid pressurization influences crack tip processes during dynamic rupture. Geophysical Research Letters 38, L24314-1–L24314-6.

Broberg, K.B., 2006. Differences Between Mode I and Mode II Crack Propagation. Pure and Applied Geophysics 163, 1867-1879.

Burridge, R., 1973. Admissible Speeds for Plane-Strain Self-Similar Shear Cracks with Friction but Lacking Cohesion. Geophysical Journal of the Royal Astronomical Society 35, 439–455.

Ougier-Simonin, A., Zhu, W., 2015. Effect of Pore Pressure Buildup on Slowness of Rupture Propagation. Journal of Geophysical Research: Solid Earth 120, 7966–7985.

Psakhie, S.G., Dimaki, A.V., Shilko, E.V., Astafurov, S.V., 2016. A coupled discrete element-finite difference approach for modeling mechanical response of fluid-saturated porous materials // International Journal for Numerical Methods in Engineering 106, 623–643.

Psakhie, S.G., Shilko, E.V., Popov, M.V., Popov, V.L., 2015. The Key Role of Elastic Vortices in the Initiation of Intersonic Shear Cracks // Physical Review E 91, 063302-1–063302-6.

Psakh'e, S.G., Zol'nikov, K.P., 1997. Anomalously High Rate of Grain Boundary Displacement Under Fast Shear Loading. Technical Physics Letters 23, 555–556.

Radi, E., Loret, B., 2007. Mode II intersonic crack propagation in poroelastic media. International Journal of Fracture 147, 235–267.

Shilko, E.V., Psakhie, S.G., 2014. Theoretical Study of Peculiarities of Unstable Longitudinal Shear Crack Growth in sub-Rayleigh and Supershear Regimes. AIP Conference Proceedings 1623, 571–574.

Shilko, E.V., Psakhie, S.G., Popov, V.L., 2015. Parametric Study of the Conditions of Supershear Crack Propagation in Brittle Materials. AIP Conference Proceedings 1683, 020209-1–020209-4.

Svetlizky, I., Pino Munoz, D., Radiguet, M., Kammer, D.S., Molinary, J.-F., Fineberg, J., 2016. Properties of the Shear Stress Peak Radiated Ahead of Rapidly Accelerating Rupture Fronts That Mediate Frictional Slip. Proceedings of the National Academy of Sciences of the United States of America 113, 542–547.

Wong, T.-F., Baud, P., 2012. The brittle-ductile transition in porous rock: A review. Journal of Structural Geology 44, 25–53.